



Published in final edited form as:

*J Med Chem.* 2005 June 2; 48(11): 3714–3728.

## Decoys for Docking

Alan P. Graves<sup>†,‡</sup>, Ruth Brenk<sup>†</sup>, and Brian K. Shoichet<sup>\*,†</sup>

*Department of Pharmaceutical Chemistry, Graduate Group in Biophysics, University of California San Francisco, 1700 4th Street, San Francisco, California 94143-2550*

### Abstract

Molecular docking is widely used to predict novel lead compounds for drug discovery. Success depends on the quality of the docking scoring function, among other factors. An imperfect scoring function can mislead by predicting incorrect ligand geometries or by selecting nonbinding molecules over true ligands. These false-positive hits may be considered “decoys”. Although these decoys are frustrating, they potentially provide important tests for a docking algorithm; the more subtle the decoy, the more rigorous the test. Indeed, decoy databases have been used to improve protein structure prediction algorithms and protein–protein docking algorithms. Here, we describe 20 geometric decoys in five enzymes and 166 “hit list” decoys—i.e., molecules predicted to bind by our docking program that were tested and found not to do so—for  $\beta$ -lactamase and two cavity sites in lysozyme. Especially in the cavity sites, which are very simple, these decoys highlight particular weaknesses in our scoring function. We also consider the performance of five other widely used docking scoring functions against our geometric and hit list decoys. Intriguingly, whereas many of these other scoring functions performed better on the geometric decoys, they typically performed worse on the hit list decoys, often highly ranking molecules that seemed to poorly complement the model sites. Several of these “hits” from the other scoring functions were tested experimentally and found, in fact, to be decoys. Collectively, these decoys provide a tool for the development and improvement of molecular docking scoring functions. Such improvements may, in turn, be rapidly tested experimentally against these and related experimental systems, which are well-behaved in assays and for structure determination.

### Introduction

Molecular docking is widely used to predict novel ligands for molecular targets.<sup>1–14</sup> In such applications, a large database of organic molecules is screened against a binding site, typically on a protein. These database compounds are often readily available either from vendors or from internal collections. The docked molecules are sampled in multiple conformations and orientations within the binding site, and each configuration is scored for complementarity to the receptor. The best scoring protein–ligand complexes are saved and ranked relative to the rest of the small molecule database. These best ranking compounds or “hits” can be tested experimentally for binding to the target. Ideally, all would bind with reasonable affinity, but typically, most compounds tested fail to bind. In work from this lab, for example, 56 compounds predicted to inhibit  $\beta$ -lactamase were tested experimentally, with three of these proving to be true inhibitors. Although often structurally similar to these three novel inhibitors, the other 53 compounds were false positives or “decoys”.<sup>15</sup> Similarly, of 365 molecules predicted as high-

\* To whom correspondence should be addressed. Tel: 415-514-4126. Fax: 415-514-1460. E-mail: shoichet@cgl.ucsf.edu..

<sup>†</sup>Department of Pharmaceutical Chemistry.

<sup>‡</sup>Graduate Group in Biophysics.

**Supporting Information Available:** A list of protein–ligand complex structures from the PDB used to test for geometric decoys, DOCK score vs RMSD bounding plots for each protein–ligand complex, a list of experimentally tested ligands and decoys for L99A, L99A/M102Q, and AmpC, and crystal statistics for catechol in complex with L99A/M102Q. This material is available free of charge via the Internet at <http://pubs.acs.org>.

ranking hits for PTP1B, 238 (65%) were decoys.<sup>16</sup> This range of hit rates is not uncommon for the field.<sup>17–19</sup>

Docking screens have had an impact, notwithstanding these high failure rates, because of their focus on easily available compounds. Thus, whereas the false positives are frustrating, they are tolerable. The idea we will develop here is that docking decoys are not only tolerable, but they can be actually useful for testing and improving docking algorithms. With the right controls and in the right context, they highlight particular weaknesses of an algorithm.

In making this argument, we steal a leaf from work on protein–structure prediction and protein–protein docking.<sup>20–31</sup> In these fields, as in small molecule docking and virtual screening, the challenge is to distinguish the native structure from reasonable, but incorrect, alternatives. This is difficult because of the fine balance between solvated and folded (or bound) states and because of the many configurations and conformations accessible to proteins. Databases of decoy structures have been helpful in refining folding scoring functions by explicitly presenting them with some of the more reasonable of those possible alternative structures. Thus, in protein structure prediction, the Park and Levitt decoy sets,<sup>20</sup> the EMBL decoy sets,<sup>32</sup> and the ROSETTA decoy set<sup>22</sup> are widely used to test new scoring methods. Protein complex decoy sets<sup>31,33</sup> have been used to a similar effect.<sup>29</sup> The same logic underlying these folding and protein–protein decoys should apply to virtual screening, whose first task is to separate likely geometries and likely molecules from their decoy alternatives.

Because molecular docking aims to identify the correct conformations and orientations of known ligands, as well as predict novel ones, we will consider two types of decoys. The simplest are geometric decoys, where docking predicts an incorrect configuration of a ligand in a binding site. Hit list decoys address the second and arguably more complicated problem of distinguishing true binders from nonbinders for a target. These hit list decoys rank highly in docking screens and are predicted to bind but, on experimental testing, are found not to bind at relevant concentrations.

We will consider geometric decoys for five well-characterized enzymes: dihydrofolate reductase (DHFR), thymidylate synthase (TS), purine nucleoside phosphorylase (PNP), acetylcholine esterase (AChE), and thrombin–77 complexes are considered overall. For each system, we find several cases where the docked geometry is correct and several where the best-docked geometry is a decoy. We define a geometric decoy to be a configuration that scores better than the native geometry and that deviates more than 3.0 Å root mean square deviation (RMSD) from the crystallographic configuration thus failing to make key interactions with the binding pocket. For hit list decoys, we investigate molecules tested as ligands for three well-studied binding sites. Two are cavities in the core of T4 lysozyme that are small, well-defined, and completely sequestered from bulk solvent. The first of these, created by the substitution Leu99 to Ala (Leu99 → Ala mutant of T4 lysozyme, L99A) in the core of the protein,<sup>34</sup> opens a small, uniformly hydrophobic, solvent inaccessible cavity that binds small aryl hydrocarbons, such as benzene, indene, and naphthalene but few molecules larger. A second substitution in this site, Met102 to Gln (Leu99 → Ala and Met102 → Gln double mutant of T4 lysozyme, L99A/M102Q), introduces a single polar atom, the O $\epsilon$  of Gln102, into the cavity. This polar cavity binds, in addition to the apolar aryl hydrocarbons recognized by L99A, more polar molecules such as phenol and aniline derivatives, which do not bind to L99A.<sup>35</sup> The great advantage of these cavity sites is that they are so simple that when a decoy is predicted, the reason it is a decoy is fairly obvious. We will consider 46 decoys for L99A and 24 decoys for L99A/M102Q cavities. Each of these decoys, which scored well by the DOCK3.5.54 scoring function, may be compared to the 56 and 78 known ligands, and the nine and 12 crystal structures, for the apolar and polar cavities, respectively. Our third model system is a real drug target, AmpC  $\beta$ -lactamase. We will consider 84 decoy molecules predicted for  $\beta$ -lactamase,

which may be compared to 26 ligands for this enzyme. In addition, the predictions made for L99A, L99A/ M102Q, and  $\beta$ -lactamase can easily be tested experimentally, thus adding to the value of these as model systems for testing and comparing docking algorithms.

Of course, it might be argued that our decoys reflect pathologies of the DOCK scoring function and are not generally interesting for the field. We will therefore evaluate these decoys with five other docking scoring functions including ScreenScore,<sup>36</sup> FlexX,<sup>37</sup> PLP,<sup>38</sup> PMF,<sup>39</sup> and SMOG2001.<sup>40</sup> Whereas DOCK is a force field-based scoring function, ScreenScore, FlexX, and PLP are empirical scoring functions, which are derived from assigning experimentally determined binding free energies into different additive contributions such as the number of hydrogen bonds, ionic interactions, apolar contacts, and entropy penalties for fixing rotatable bonds in docking the ligand onto the receptor.<sup>41</sup> PMF and SMOG2001 are knowledge-based scoring functions, which use statistical analyses of three-dimensional complex structures to derive a sum of potentials of mean force between receptor and ligand atoms.<sup>41</sup> Brooks et al. carried out a study where they compared force field, empirical, and knowledge-based scoring functions using crystallographic and geometric decoy geometries of 189 protein–ligand complexes.<sup>42</sup> While comprehensive, that study did not include comparisons of scoring functions against virtual screening experiments that include ligands and nonbinders or hit list decoys. Our results support the notion that each of the scoring functions that we tested, including our own, are prone to decoys even against the very simple cavity sites. We will argue that these decoys identify specific problems with each docking scoring function.

## Results

### Geometric Decoys

We selected five well-characterized proteins each having several ligand-bound structures in the Protein Data Bank (PDB) to test the ability of a particular scoring function to reproduce the crystallographic or “native” ligand geometries in their cognate proteins. All of the ligands for a particular protein were initially docked against one representative protein structure. These “cross-docking” calculations assume that there is only a small conformational change in the protein upon binding different ligands. This rigid treatment of the protein is often used when docking a large compound database. Decoys were also docked to their native protein structures to ensure that they were not simply the product of a “wrong” protein conformation—only decoys that passed this test are listed. When docking against any structure, we also ensured that sufficient sampling of the ligand took place to find poses very close to that determined by crystallography, regardless of their scores (Supporting Information). We considered 19 complexes of DHFR, which is a key enzyme in folate biosynthesis; 25 complexes of thrombin, a target for anticoagulant drug therapy; 12 complexes of PNP, which is a critical enzyme in the purine salvage pathway; 13 complexes of TS, a well-studied target for anticancer drug design; and eight complexes of AChE, which is a target for drugs for the management of Alzheimer’s (Supporting Information). DOCK3.5.54 was used to generate and score multiple conformations and orientations of each ligand in its cognate protein. In most cases, the best scoring ligand geometries matched the crystallographic ligand geometries to within 2.0 Å RMSD; such geometries were considered to be native-like. We focused on ligands that had decoy geometries (>3.0 Å RMSD from the native pose with better energy scores than any of the natively dockings) to develop a test set of geometric decoys. DOCK predicted four geometric decoys for DHFR, five for thrombin, two for PNP, six for TS, and three for AChE (Table 1 and Supporting Information).

To investigate how robust these geometric decoys were, we also evaluated the poses sampled by DOCK-3.5.54 with five scoring functions used in molecular docking—ScreenScore, FlexX, PLP, PMF, and SMOG. We note that these scoring functions were used as deployed in a stand alone rescoring program (Dr. Martin Stahl, Basel) and may differ from the current state of these

scoring functions as they exist in their native programs, although we expect differences to be relatively small. We used these scoring functions to rescore the predicted geometries for two geometric decoys and two well-matched ligands from each of the five proteins–20 complexes overall (Table 1). Although not reported here, in every case, the crystallographic pose score for each scoring function was higher (worse) than the energy of the best scoring pose for each scoring function; all decoys are scoring decoys, not sampling decoys. In general, these scoring functions, with the exception of SMOG, performed no worse than DOCK in those complexes where DOCK found a natively high scoring pose. For about half of the geometric decoys found by DOCK, these other scoring functions, again with the exception of SMOG, correctly scored native poses better than decoys (Table 1).

We tested the notion that we could improve DOCK's ability to distinguish native geometries from decoy geometries by softening DOCK's van der Waals potential and by increasing the weight of DOCK's electrostatic score. We softened DOCK's hard 12–6 van der Waals potential to an 8–6 potential to reduce the effect of close contacts between native protein–ligand geometries determined by crystallography. We additionally weighted the electrostatic interaction energy from DOCK by a factor of four to simulate the importance of hydrogen bonds. For four out of 10 of DOCK's geometric decoys (Table 1), the native geometry was salvaged from the decoy geometries by using the softer van der Waals potential and an increased weight for the electrostatic score. This softer DOCK scoring function only failed on one of the native-like dockings (Table 1). The consequences of this change on hit list decoys were less promising (below).

### Hit List Decoys

To investigate hit list decoys, we turned to two well-characterized cavity sites, the L99A and L99A/M102Q lysozyme mutants, and one well-characterized drug target, AmpC  $\beta$ -lactamase (Figure 1). The cavity sites bind mostly small, aromatic hydrocarbons with affinities ranging from 10 to about 500  $\mu$ M. Molecules are frequently tested for binding in the millimolar concentration range, the major limitations being solubility and, for initial spectral determinations of binding, optical density. For  $\beta$ -lactamase, the known, noncovalent ligands bind with affinities between 14 and 700  $\mu$ M; molecules with IC<sub>50</sub> values better than 5 mM can be detected, as long as solubility does not interfere (it typically does not in the series of ligands found to date). DOCK was used to screen about 200 000 compounds of the Available Chemicals Directory (ACD) against these sites. The screened database contained 49, 70, and 26 known ligands for L99A, L99A/M102Q, and AmpC, respectively.

Of the 49 known ligands for the hydrophobic cavity L99A in the ACD,<sup>35,43</sup> 39 were predicted by DOCK to score in the top 10 000, which constitutes the top 5% of the docked database of 200 000 molecules. Their ranks ranged from 21 to 9880, with 17 in the top 500, or approximately the top 0.25%, of the database (Table 2). There are 45 known nonbinders to L99A,<sup>35,43,44</sup> 22 of which scored in the top 10 000 with ranks from 46 to 8243 (Table 3). Ten of these scored in the top 500 of the database. There were many others from the top of the hit list that looked like either ligands or nonbinders. Of the latter, an additional eight suspected decoys were tested experimentally and found not to bind detectably to the protein: That is, they were confirmed as decoys (compounds **5–10**, **13**, and **19** in Table 3). Taking into account these new experimental results, a total of 17 decoys scored in the top 500 ranked compounds, and 30 decoys scored in the top 10 000.

A slightly more complex cavity is that of L99A/M102Q, which introduces a single polar atom into the otherwise apolar cavity. There were 78 ligands for L99A/M102Q, 55 of which scored in the top 10 000 of the database—in accordance with the observation that the L99A ligands toluene and benzene also bind to the L99A/M102Q site, we assumed that the 56 known ligands of L99A also bind to this more polar site (Tables 2 and 4).<sup>35</sup> Of these ligands, 15 scored in the

top 500, or the top 0.25%, of the database (Table 4). There were four known nonbinders that scored in the top 10 000,<sup>45</sup> none of which scored in the top 500. Nevertheless, many of the molecules that ranked in the top 500 looked like decoys. Seven of these were experimentally tested, and six showed no evidence of binding to the polar cavity (compounds **1–6**, Table 4). Somewhat to our surprise, one compound, catechol, which we thought would not bind because of excess polarity, does bind to the polar cavity. To understand its basis for binding, we determined the structure of catechol in complex with L99A/ M102Q to 1.55 Å resolution by X-ray crystallography (Figure 2). The data suggest two binding modes for catechol. In the first mode, one phenol oxygen of catechol is 2.63 Å and the second is 5.35 Å from the O $\epsilon$  of Q102 as shown in Figure 2. Positive  $F_o - F_c$  density contoured at 3 $\sigma$  (green mesh; Figure 2) at the three-position carbon of catechol (Figure 2) suggests a second binding mode in which catechol has rotated 60° counterclockwise with respect to the first binding mode, and the two phenol oxygens are 2.51 and 2.66 Å from the O $\epsilon$  of Q102 (not shown).

We were interested in how the other five scoring functions, ScreenScore, FlexX, PLP, PMF, and SMOG, would rank the L99A and L99A/M102Q ligands and decoys. Using these functions, we rescored the top 10 000 ranking compounds against each of the two cavities (Tables 2–4). The ranks for 28 out of 39 of the known ligands for L99A that score in the top 10 000 are worsened by three or more of the other scoring functions, as were the ranks of 25 out of 30 of the known decoys. Similarly, when ScreenScore, FlexX, PLP, PMF, and SMOG were used to rescore the top 10 000 scoring compounds against the polar cavity (L99A/M102Q), the ranks of 15 out of 22 of the known binders were lowered by three or more of the scoring functions, as were the ranks of seven out of 10 of the decoys. Although the ranks of both ligands and decoys were lowered by these other scoring functions, the ranks of the ligands fell further (were ranked worse) than those of the decoys. This is reflected in the overall enrichment factors of the ligands for the different scoring functions against the two cavity sites (Figure 3).

If both ligands and decoys ranked worse by Screen-Score, FlexX, PLP, PMF, and SMOG, a reasonable question is what molecules ranked better? We examined the compounds that ScreenScore, FlexX, PLP, PMF, and SMOG ranked highly (Table 5). To our eyes, the top scoring compounds for these scoring functions typically looked too polar or too large or both. For instance, many of the very top scoring molecules for the hydrophobic L99A cavity sported multiple hydrogen bonding groups (Figure 4). Of course, our biases here might be wrong. We therefore tested compounds ranked among the top 10 hits for each of the five scoring functions against L99A and L99A/M102Q (17 compounds in total—several were predicted by multiple scoring functions) (Table 5). Of these 17, none were found to bind when tested.

To test the hypothesis that a permissive treatment of steric contacts and an increased emphasis on polar interactions result in worse enrichment of ligands when docking against a large database of decoys, we rescored the top 10 000 hits from both cavity sites by using the altered DOCK score, which combined a softened 8–6 van der Waals potential and an increased weight for the electrostatic interaction energy. This scoring function, which had improved performance vs the geometric decoys, enriched fewer ligands for both cavity sites in the top 1% or top 1000 compounds of the database (Figure 3). As compared to the standard DOCK scoring function, the “softened” DOCK scoring function ranked 13 out of 42 L99A and six out of 17 M102Q decoys higher. Beyond the top 1–2% of the database, the altered DOCK scoring function improved enrichment of ligands as compared to the standard DOCK score. However, this is mostly because we dock against a single, relatively small conformation of the cavities, which cannot easily accommodate some of the larger known ligands in the database without conformational change.

To investigate decoys for a real druggable binding site, we turned to the enzyme  $\beta$ -lactamase, a well-studied target for antibiotic resistance. Unlike the lysozyme cavities, but like most drug

targets, the active site of this enzyme presents a mixture of polar and nonpolar functionality, is large, and has an extensive solvent interface. There are 26 known noncovalent ligands for AmpC (ref 6 and Morandi, Tondi, and Shoichet, unpublished) and 76 known decoy hits from a screen of the ACD database—23 of these decoys were tested for this paper, and 53 had been previously discovered (Table 6).<sup>15</sup> All of the ligands and 65 of the decoys scored in the top 20 000, or approximately 10%, from an ACD screen against the AmpC structure. The ligands ranked from three to 11 740, with five in the top 500 (Table 6). The decoys ranked from 10 to 9344 with 26 in the top 500 (Table 6). Of the 20 high scoring docking hits for AmpC tested for this paper, only one inhibited the enzyme with a  $K_i$  value of about 93  $\mu$ M (ligand 2, Table 6).

We used ScreenScore, FlexX, PLP, PMF, and SMOG to rescore the top 20 000 ranking compounds against AmpC (Table 6). As in the cavity sites, the ranks for most of the ligands and decoys were lowered. The ranks for 22 out of 26 of the ligands for AmpC that score in the top 20 000 are worsened by three or more of the other scoring functions, as were the ranks of 45 out of 67 of the decoys (Table 6). We then considered the compounds that ScreenScore, FlexX, PLP, PMF, and SMOG ranked highly (Table 7). As in the cavity sites, we tested compounds ranked among the top ranking hits for each of the five scoring functions. Eleven compounds in total—several were predicted by multiple scoring functions—were experimentally tested (Table 7). None of these 11 compounds were found to bind when tested. The “softened” DOCK scoring function was also used to rescore the top 20 000 ranking compounds against AmpC. As in the cavity sites, the less permissive DOCK scoring function enriched fewer known AmpC ligands in the top 1% of the database screen. Figure 3C compares the overall enrichment factors of the known ligands for each scoring function.

Two caveats of our results should be considered. First, we only use DOCK generated poses of compounds rather than fully redocking with the other docking programs, which would allow them to generate as well as score ligand poses. It may be that the geometric decoys for these other scoring functions would not have been found if we had allowed them to both sample and score docking poses, because they would have found native-like geometries that DOCK missed. However, we did generate many low RMSD poses regardless of score so at least we can say that many native poses were sampled. Moreover, we note that by and large these other scoring functions did better than our own with the geometric decoys. For the hit lists, we only use the other scoring functions to rescore the best scoring DOCK pose. Here, too, we know that many true ligands are in the hit lists, in near native geometries, so this is not a question of the right molecules not being available to rank well— they are present. Nor is it a question of gross bias on our part on what may or may not be a ligand or a decoy since several of the best ranking compounds for L99A, L99A/M102Q, and AmpC predicted by the other scoring functions were tested experimentally and found not to bind. The second caveat pertains to how good we are at experimentally distinguishing ligands from decoys. For the two cavity sites, a ligand is a molecule that binds at concentrations of a few millimolar or lower—molecules that might in fact bind at higher concentrations cannot be detected often for solubility or spectral density reasons and so are considered decoys. Similarly, for AmpC, we can detect molecules that bind in the 10 mM range; molecules that might bind at higher concentrations will be considered decoys. The range of affinities for known purely noncovalent AmpC ligands is between 1  $\mu$ M and 1 mM. The range for the cavity ligands is between 10  $\mu$ M and about 2 mM.

## Discussion

From a practical standpoint, virtual screening may be considered successful if even 10% of predicted ligands bind to the target at relevant concentrations. From a scientific standpoint, such a failure rate is disconcerting, all the more so since we typically cannot attribute it to a single algorithmic failure. We argue that, with the proper controls and in the proper systems,

the decoy molecules that make up the high failure rate of docking screens are informative, arguably more so than successful predictions from docking. Three points stand out from this study. First, all six scoring functions that we tested, including our own, were prone to decoys, often obvious ones. Second, the ability to distinguish geometric decoys from native structures was not correlated with performance on hit list decoys. Third, the model systems discussed here lend themselves to simple experiments, allowing a cycle of algorithmic development followed by prospective testing.

A startling aspect of the decoys is how obvious many of them are. This is most clearly seen in the cavity sites. Molecules such as phenol (ranked 235 by DOCK out of over 200 000 molecules docked, decoy 12, Table 3), diaminophenol (ranked 1st by the FlexX scoring function, decoy 5, Table 5), and 8-aminoquinoline (ranked 3rd by the PMF scoring function, decoy 3, Table 5) are too polar to bind to the buried, completely hydrophobic L99A cavity (Figure 1). Such molecules have little or no chance of making hydrogen bonds in this site, yet must be desolvated from water. Thus, they are easy to distinguish from ligands such as benzene, which pay a much smaller desolvation penalty. Molecules such as acenaphthylene (ranked 4th by the SMOG scoring function, decoy 4, Table 5) are too large for the cavities. That these decoys were, nevertheless, among the very top ranking hits from among the docking scoring functions indicates that they are too permissive to steric violations, desolvation penalties, and frequently both. Why are these violations permitted?

One answer is that these functions may have been devised as initial screens, envisioning more sophisticated secondary calculations to weed out the sorts of decoys that we find here. Thus, a scoring function might be intentionally permissive to steric violations, implicitly allowing for receptor conformational accommodation that could be properly evaluated with a full energy minimization or molecular dynamics treatment. Such calculations are too costly during a database screen but might be considered for a smaller list of initial hits. The cost of such permissiveness is to allow decoy molecules as high ranking hits, to the point that they might crowd out true ligands from the small number of hits possible to reevaluate with the more sophisticated functions.

Consideration of the performance of the scoring functions on the geometric decoys hints, however, at another explanation for the hit list decoys. Most scoring functions did relatively well on the geometric decoys, distinguishing the native from the decoy poses for most of the 20 complexes that we investigated. Docking scoring functions have been extensively tested for their ability to reproduce ligand geometries observed in experimental structures.<sup>18,42</sup> Indeed, many have been parametrized based on the interactions observed in experimental structures.<sup>37–40</sup> This is similar to protein folding functions parametrized on the interactions in the folded structures of proteins. In folding, it was realized that it is important to consider not only observed interactions but also possible decoy interactions—this has led to the construction of sets of decoy folds by which folding functions are now tested.<sup>20–23</sup> In small molecule docking, decoys have not been considered in parametrization, at least not formally, and this may have led to an overemphasis on certain interactions and an allowance for certain violations. In parametrizing to reproduce experimental geometries, for instance, one will do well to heavily weight polar interactions, such as hydrogen bonds, which impart directional specificity. Similarly, because steric violations are sometimes present in experimental structures, it is sensible to be permissive to steric repulsion. Such emphasis and allowances can cause problems that only become apparent in a virtual screening application. Whereas polar interactions are key to proper positioning of a molecule, their net contribution to binding affinity is often modest. A scoring function that is heavily biased toward polar interactions may overemphasize polar hits from docking screens, such as diaminophenol, aminoquinoline, and pterin as ligands for the hydrophobic cavity in lysozyme. Similarly, permissiveness to steric violations will favor larger decoys at the expense of smaller ligands in a database screen.

To test the effect of more sterically permissive and more polar scoring functions on geometric and hit list decoys, we increased the permissiveness to steric violations in the DOCK scoring function and increased the weight of the electrostatic score by 4-fold. This change salvaged four of 10 of our geometric decoys (Table 1). Conversely, in database docking against the cavity sites, significantly fewer ligands were found in the top 1000–2000 ranking hits than were found by the standard, less permissive DOCK scoring function (Figure 3A,B). Thus, whereas a scoring function that is sterically permissive and that emphasizes polar interactions may do well for reproducing crystal structures, the very same function may do worse in database screens.

How extendable are these observations to docking screens against “real” binding sites? The decoys and ligands found for AmpC  $\beta$ -lactamase bear out trends in the toy sites, although admittedly this site, like all real sites, is complex enough to defeat single explanations for decoys. As in the cavity sites, each scoring function predicts several decoys (Table 7). DOCK’s predicted decoys are ranked poorly by most of the other scoring functions (Table 6), and the enrichment of known ligands is worse for the other scoring functions, including the less permissive DOCK scoring function (Figure 3C); alternatively, the other scoring functions have decoys that are ranked poorly by DOCK (Table 7). With the exception of decoys 1 and possibly 4, most of these decoys look unlike the known AmpC ligands. Here, too, the decoys are obviously different from the ligands.

Whereas many of the decoys for both the cavity sites and the  $\beta$ -lactamase were obvious, some were fairly subtle. For instance, catechol (ligand 11, Table 4) is a ligand for L99A/M102Q, but 2-aminophenol, which replaces a single hydroxyl group with an amino group, is a decoy (decoy 6, Table 4). We were surprised enough by this difference to determine the structure of the catechol complex by X-ray crystallography. The electron density of this 1.55 Å structure suggests that catechol has two binding modes in the cavity (Figure 2). Either binding mode in principle would be accessible to 2-aminophenol. A likely reason that 2-aminophenol does not bind is that its amino group is a strong hydrogen bond donor as compared to catechol’s phenolic oxygens, which are fairly weak hydrogen bond acceptors; therefore, the cost of desolvation and binding of 2-aminophenol to M102Q is likely greater than that of catechol. Without experimental binding or structural data, slight differences such as those between catechol and 2-aminophenol can easily be overlooked by even a trained biochemist, not to mention a docking scoring function.

We conclude by returning to the obviousness of many of the hit list decoys, including the decoys returned by our own docking program. Whereas this might seem to be a depressing result, we draw some comfort from it. Docking screens have, after all, predicted novel ligands for many receptors,<sup>1–11</sup> notwithstanding their propensity to decoys. What we find encouraging is that fairly simple improvements to docking scoring functions might remove these obvious decoys. Of course, it is possible to treat one type of decoy and introduce another, but in experimentally tractable systems, this may be easily tested. We thus hope that the decoy molecules and geometries described here will be useful to the field, leading to a cycle of development and testing in these and other model systems.

## Materials and Methods

### Protein and Ligand Preparation for Single Ligand Docking

Ligand-bound protein complexes for each of the five enzymes—19 complexes for DHFR, 25 complexes for thrombin, 13 complexes for TS, 12 complexes for PNP, and eight complexes for AChE—were obtained from the PDB (Table 1 and Supporting Information). One representative complex from each enzyme was chosen as the template for docking. 3DFR was chosen for DHFR, 1A4W was chosen for thrombin, 2BBQ was chosen for TS, 1B8O was



chosen for PNP, and 1E66 was chosen for AChE. The complexes were then superimposed onto their templates by matching C $\alpha$  backbone atoms of well-defined secondary structural elements. This alignment had no influence on scoring of the docked ligands; it merely simplified the comparison of docked and crystallographic geometries. The resulting matched ligands were then copied into separate files for further preparation. Protons were added to the ligands, and atomic partial charges were computed using SYBYL (Tripos, St. Louis, MO). The ligands were converted from pdb to mol2 format. Atom types and bond orders were checked for accuracy, and a docking database for each ligand was prepared from the mol2 formatted ligands. Conformations of each ligand were generated using Omega 0.9 (OpenEye Scientific Software, Santa Fe, NM) and stored in a multiconformer database.<sup>46</sup> Partial atomic charges, solvation energies,<sup>35</sup> and van der Waals parameters<sup>47</sup> were calculated as previously described. The protein structures were prepared for docking as described.<sup>48</sup>

### Molecular Docking of Geometric Decoys

DOCK3.5.54 was used to dock the ligands to the active site of their respective model proteins. This version of DOCK samples configurations of the ligands more or less finely according to “bin” and overlap distance tolerances.<sup>49,50</sup> Ligand and receptor bins were set to 0.4–1.0 Å, and overlap bins were set to 0.0–0.4 Å; the distance tolerance for matching ligand atoms to receptor matching sites was set to 1.0–1.5 Å. Each ligand configuration was sampled for steric fit; those passing the steric filter were scored for combined electrostatic and van der Waals complementarity. In any given orientation, the high-scoring ligand conformation was minimized with 20 steps of simplex rigid-body minimization.<sup>51</sup> For each ligand–receptor complex, multiple conformations and orientations of the ligands were written out. Multiple configurations of 20 of these ligands, four from each enzyme target, were rescored using SCORE and SMOG (see below).

### Docking Screens vs L99A and L99A/M102Q Cavities and AmpC $\beta$ -Lactamase

The docking calculations for the cavities were performed as previously described<sup>35</sup> using the benzene-bound structure of L99A (181L) and the apo structure of L99A/M102Q (1LGU). The docking database was the 2000.1 version of the ACD (MDL, San Leandro, CA). Compounds containing three or more fluorine atoms as well as compounds containing more than 25 heavy atoms were removed from the database leaving 60 879 molecules in the dockable database. The docking screens for AmpC were performed as previously described<sup>15</sup> using an apo AmpC structure (1KE4). The same version of the ACD was used as the docking database without prior filtering for a total of 220 768 compounds. AMSOL<sup>52,53</sup> was used to calculate partial atomic charges for each ligand.<sup>35</sup> Conformations of each ligand were generated using Omega 0.9 (OpenEye Scientific Software) and stored in a multiconformer database.<sup>46</sup> The best scoring conformation of each of the 10 000 top scoring molecules against L99A and L99A/M102Q as well as the 20 000 top scoring molecules against AmpC were saved and rescored using SCORE and SMOG.

### Rescoring the Hit Lists with SCORE

Stand alone versions of ScreenScore, FlexX, PLP, and PMF scoring functions were implemented in the program SCORE (kindly provided by M. Stahl). SCORE allows one to evaluate any given protein–ligand configuration by each of these scoring functions. The ligand conformations generated and scored by DOCK3.5.54 were converted to SYBYL mol2 format using an atom typing script in CHIMERA.<sup>54</sup> The bond order information was then added by BABEL version 1.6 (University of Arizona). These scripts simply converted the DOCK output into mol2 format. The SCORE script was then run using the protein pdb file, the active site pdb file, and a ligand multi-mol2 file to calculate the ScreenScore, FlexX, PLP, and PMF score for each ligand conformation.

## Rescore Using SMOG

Similarly, the docked poses were rescored using the SMOG2001 scoring function (generously provided by B. Dominy and E. Shakhnovich).<sup>40</sup> SMOG uses pdb formatted ligand files, and no additional treatment of DOCK output was necessary. SMOG currently does not have the parameters for halogen atoms so those compounds containing F, Cl, Br, and I were not considered in the enrichment calculations for SMOG.

## Binding of Compounds to L99A and L99A/M102Q by Upshift of Thermal Denaturation Temperature

L99A and L99A/M102Q were prepared and purified as described.<sup>35</sup> Thermal denaturation experiments were carried out in a Jasco J-715 spectropolarimeter with a Jasco PTC-348WI Peltier-effect temperature control device and in-cell stirring. To screen the compounds for binding in their neutral forms, denaturation experiments were done at appropriate pH values: compounds 3-fluorobenzonitrile (decoy 5, Table 3), 5-bromopyrimidine (decoy 9, Table 3; decoy 5, Table 4), and 1,2,4-triazolo[1,5-a]-pyrimidine (decoy 9, Table 5) obtained from Aldrich and 1,6-naphthyridine (decoy 7, Table 5) obtained from TCI were assayed in a pH 5.4 buffer containing 100 mM sodium chloride, 8.6 mM sodium acetate, and 1.6 mM acetic acid; compounds 4-vinylpyridine (decoy 10, Table 3; decoy 4, Table 4), 1-vi-nylimidazole (decoy 13, Table 3; decoy 3, Table 4), 2-aminophenol (decoy 6, Table 4), pterin (L99A decoy 2, Table 5), and 8-aminoquinoline (L99A decoy 2, Table 5) obtained from Aldrich, compound 3,4-diaminofluorobenzene (decoy 2, Table 4) obtained from Avocado Research, compounds 4-amino-2-methylthioquinazoline (L99A decoy 1, Table 5) and 2-ami-nobenzimidazole (M102Q decoy 3, Table 5) obtained from Acros, compounds 2,5-diaminophenol (L99A decoy 5 and M102Q decoy 1, Table 5) and 7-amino-5-hydroxy-s-triazolo[1,5-a]pyrimidine (M102Q decoy 2, Table 5) obtained from Salor, compounds 4-hydrazinethieno[2,3-d]pyrimidine (L99A decoy 6 and M102Q decoy 4, Table 5) and [1,2,4]triazolo[1,5-a]-pyrimidin-7-amine (M102Q decoy 6, Table 5) obtained from Bionet, compound 3-methoxymethylindole (L99A decoy 8, Table 5) from TCI, and adenine (M102Q decoy 5, Table 5) from Sequoia were assayed in a pH 6.8 buffer composed of 50 mM potassium phosphate (a mixture of  $\text{KH}_2\text{PO}_4$  and  $\text{KH}_2\text{PO}_4$ ), 200 mM potassium chloride, and 38% (v/v) ethylene glycol; compounds 2-fluorobenzaldehyde (decoy 6, Table 3), methylchlorodifluoroacetate (decoy 7, Table 3; decoy 1, Table 4), nitrosobenzene (decoy 8, Table 3), 2-methylbenzyl alcohol (decoy 19, Table 3), catechol (ligand 11, Table 4), acenaphthylene (L99A decoy 4, Table 5), 1-naphthalenemethanol (L99A decoy 11, Table 5), 1-methylnaphthalene (L99A decoy 11, Table 5), and 2-benzylpyridine (L99A decoy 12, Table 5) obtained from Aldrich and compound 2-naphthanitrile (M102Q decoy 7, Table 5) from Acros were assayed in a pH 3 buffer containing 25 mM potassium chloride, 2.9 mM phosphoric acid, and 17 mM  $\text{KH}_2\text{PO}_4$ , as described elsewhere.<sup>43</sup>

Thermal denaturation of the protein in the presence of the compounds was monitored by circular dichroism (CD) between 223 and 234 nm (although the 223 nm wavelength is the ideal wavelength for measuring the helical signal of T4 lysozyme, the higher wavelengths, which were less affected by absorbance from some of the compounds, can be used to monitor the edge of the helical signal). For several compounds with high absorbance in the far UV region, thermal denaturation was monitored by fluorescence emission. Fluorescence was stimulated by irradiation at 280–290 nm, and thermal denaturation was measured by the intensity of the integrated emission for all wavelengths above 300 nm using a cut-on filter. Thermal melts and data fits were performed as described.<sup>35</sup> Denaturation of the apo L99A was performed in the same buffer solutions described above. Potential ligands were included at concentrations between 1 and 10 mM. Each denaturation experiment was performed at least twice.

## Enzyme Kinetics for AmpC

AmpC from *Escherichia coli* was expressed and purified to homogeneity as described.<sup>15</sup> Thirty-eight compounds were tested for binding affinity to AmpC. Ligand 2 (Table 6) was obtained from Maybridge. Table 6 decoys 1, 2, 4, and 7 were obtained from Aldrich; decoy 3 was from Bachem; decoys 5, 6, 8–11, and 17 were from Maybridge; decoys 12, 13, and 15 were from Salor; decoy 14 was from Buttpark; and decoy 16 was from Lancaster. Table 7, decoy 1, was obtained from Pfaltz and Bauer; decoy 2 was from Aldrich; decoys 3 and 8 were from Salor; decoy 4 was from Bachem; decoys 5 and 6 were from Asinex; decoys 7 and 9 were from Maybridge; decoy 10 was from Toronto; and decoy 11 was from Bionet. In addition, decoy 29 was obtained from Buttpark; decoy 30 was from TCI America; decoys 31–33 were from Asinex; decoy 34 was from Aldrich; and decoy 35 were from Timtec (Supporting Information). All were used without further purification. Kinetic measurements with AmpC were performed in 50 mM Tris buffer (pH 7.0) using nitrocefin as a substrate.<sup>15</sup> Reactions were initiated by the addition of enzyme and monitored in methacrylate cuvettes. Any compound showing inhibition was also tested in the presence of 0.01% Triton X-100, to control for promiscuous inhibition.<sup>55,56</sup> Only ligands that are classic, nonaggregation-based inhibitors are reported here.

## Crystallography

Crystals of the mutant L99A/M102Q were grown using the conditions essentially the same as described,<sup>57</sup> and belong to the space group  $P3_221$ . The crystal was soaked for 15 min in crystallization buffer containing 10 mM catechol. After soaking, the crystal was cryoprotected with Paratone-N (Hampton Research, Aliso Viejo, CA). X-ray data were collected at 110 K with an in house Raxis IV detector. Reflections were indexed, integrated, and scaled using the HKL package.<sup>58</sup> The complex structure was refined using the CNS package.<sup>59</sup> The X-ray crystal structure has been deposited in the PDB as 1XEP.

## Acknowledgements

This work is supported by GM59957 from the NIH (to B.K.S.) and Ernst Schering Research Foundation (to R.B.). We thank Dr. Martin Stahl for use of the SCORE program and Dr. Eugene Shakhnovich for use of SMOG. We thank Yu Chen, John Irwin, and Sarah Boyce for reading this manuscript and Andrej Sali and Matt Jacobson for insightful discussions. We thank Ken Dill for suggesting an investigation of decoy molecules.

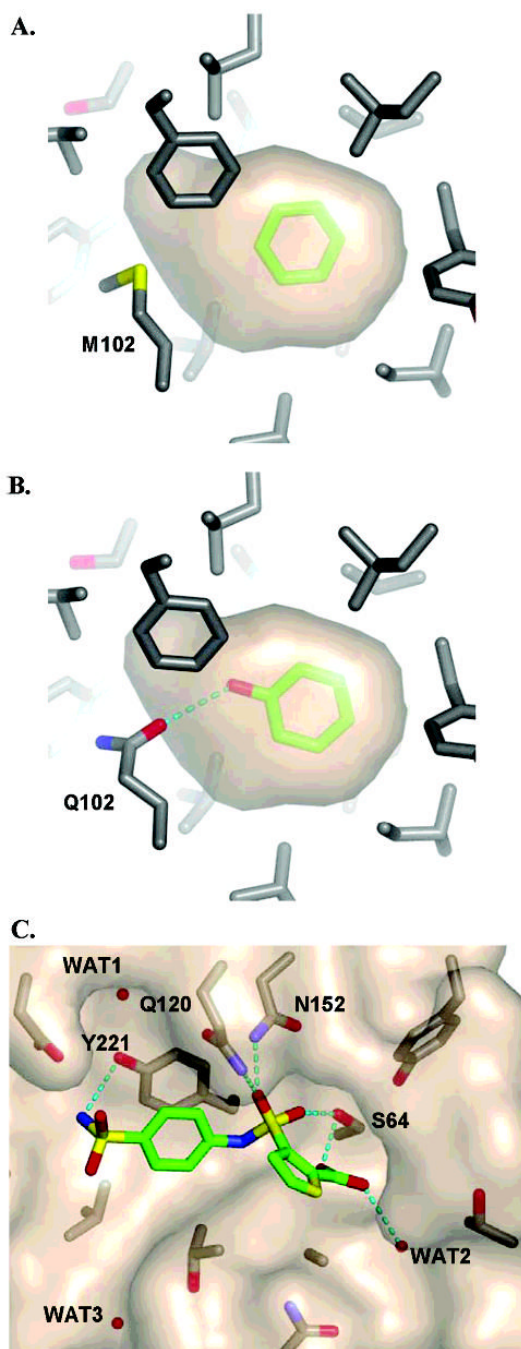
## References

1. Burkhard P, Hommel U, Sanner M, Walkinshaw MD. The discovery of steroids and other novel FKBP inhibitors using a molecular docking program. *J Mol Biol* 1999 28;7:853–858. [PubMed: 10222195]
2. Enyedy IJ, Ling Y, Nacro K, Tomita Y, Wu X, Cao Y, Guo R, Li B, Zhu X, Huang Y, Long YQ, Roller PP, Yang D, Wang S. Discovery of small-molecule inhibitors of Bcl-2 through structure-based computer screening. *J Med Chem* 2001;44:4313–4324. [PubMed: 11728179]
3. Gradler U, Gerber HD, Goodenough-Lashua DM, Garcia GA, Ficner R, Reuter K, Stubbs MT, Klebe G. A new target for shigellosis: rational design and crystallographic studies of inhibitors of tRNA-guanine transglycosylase. *J Mol Biol* 2001;306:455–467. [PubMed: 11178905]
4. Honma T, Hayashi K, Aoyama T, Hashimoto N, Machida T, Fukasawa K, Iwama T, Ikeura C, Ikuta M, Suzuki-Takahashi I, Iwasawa Y, Hayama T, Nishimura S, Morishima H. Structure-based generation of a new class of potent Cdk4 inhibitors: New de novo design strategy and library design. *J Med Chem* 2001;44:4615–4627. [PubMed: 11741479]
5. Liebeschuetz JW, Jones SD, Morgan PJ, Murray CW, Rimmer AD, Roscoe JM, Waszkowycz B, Welsh PM, Wylie WA, Young SC, Martin H, Mahler J, Brady L, Wilkinson K. PRO\_SELECT: Combining structure-based drug design and array-based chemistry for rapid lead discovery. 2. The development of a series of highly potent and selective factor Xa inhibitors. *J Med Chem* 2002;45:1221–1232. [PubMed: 11881991]

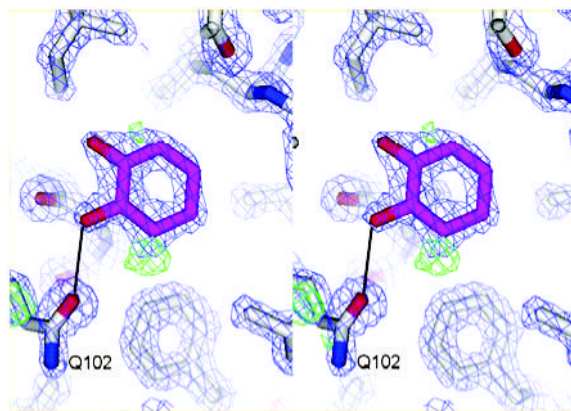
6. Ealick SE, Babu YS, Bugg CE, Erion MD, Guida WC, Montgomery JA, Secrist JA. 3rd Application of crystallographic and modeling methods in the design of purine nucleoside phosphorylase inhibitors. *Proc Natl Acad Sci USA* 1991;88:11540–11544. [PubMed: 1763067]
7. Iwata Y, Arisawa M, Hamada R, Kita Y, Mizutani MY, Tomioka N, Itai A, Miyamoto S. Discovery of novel aldose reductase inhibitors using a protein structure-based approach: 3D-database search followed by design and synthesis. *J Med Chem* 2001;44:1718–1728. [PubMed: 11356107]
8. Paiva AM, Vanderwall DE, Blanchard JS, Kozarich JW, Williamson JM, Kelly TM. Inhibitors of dihydrodipicolinate reductase, a key enzyme of the diaminopimelate pathway of *Mycobacterium tuberculosis*. *Biochim Biophys Acta* 2001;1545:67–77. [PubMed: 11342032]
9. DesJarlais RL, Seibel GL, Kuntz ID, Furth PS, Alvarez JC, Ortiz de Montellano PR, DeCamp DL, Babe LM, Craik CS. Structure-based design of nonpeptide inhibitors specific for the human immunodeficiency virus 1 protease. *Proc Natl Acad Sci USA* 1990;87:6644–6648. [PubMed: 2204060]
10. Boehm HJ, Boehringer M, Bur D, Gmuender H, Huber W, Klaus W, Kostrewa D, Kuehne H, Luebbbers T, Meunier-Keller N, Mueller F. Novel inhibitors of DNA gyrase: 3D structure based biased needle screening, hit validation by biophysical methods, and 3D guided optimization. A promising alternative to random screening. *J Med Chem* 2000;43:2664–2674. [PubMed: 10893304]
11. Grzybowski BA, Ishchenko AV, Kim CY, Topalov G, Chapman R, Christianson DW, Whitesides GM, Shakhnovich EI. Combinatorial computational method gives new picomolar ligands for a known enzyme. *Proc Natl Acad Sci USA* 2002;99:1270–1273. [PubMed: 11818565]
12. Rao MS, Olson AJ. Modelling of factor Xa-inhibitor complexes: A computational flexible docking approach. *Proteins: Struct, Funct, Genet* 1999;34:173–183. [PubMed: 10022353]
13. Vangrevelinghe E, Zimmermann K, Schoepfer J, Portmann R, Fabbro D, Furet P. Discovery of a potent and selective protein kinase CK2 inhibitor by high-throughput docking. *J Med Chem* 2003;46:2656–2662. [PubMed: 12801229]
14. Verras A, Kuntz ID, Ortiz de Montellano PR. Computer-assisted design of selective imidazole inhibitors for cytochrome p450 enzymes. *J Med Chem* 2004;47:3572–3579. [PubMed: 15214784]
15. Powers RA, Morandi F, Shoichet BK. Structure-based discovery of a novel, noncovalent inhibitor of AmpC beta-lactamase. *Structure (Camb)* 2002;10:1013–1023. [PubMed: 12121656]
16. Doman TN, McGovern SL, Witherbee BJ, Kasten TP, Kurumbail R, Stallings WC, Connolly DT, Shoichet BK. Molecular docking and high-throughput screening for novel inhibitors of protein tyrosine phosphatase-1B. *J Med Chem* 2002;45:2213–2221. [PubMed: 12014959]
17. Abagyan R, Totrov M. High-throughput docking for lead generation. *Curr Opin Chem Biol* 2001;5:375–382. [PubMed: 11470599]
18. Wang R, Lu Y, Wang S. Comparative evaluation of 11 scoring functions for molecular docking. *J Med Chem* 2003;46:2287–2303. [PubMed: 12773034]
19. Perola E, Walters WP, Charifson PS. A detailed comparison of current docking and scoring methods on systems of pharmaceutical relevance. *Proteins* 2004;56:235–249. [PubMed: 15211508]
20. Park B, Levitt M. Energy functions that discriminate X-ray and near native folds from well-constructed decoys. *J Mol Biol* 1996;258:367–392. [PubMed: 8627632]
21. Mirny LA, Shakhnovich EI. How to derive a protein folding potential? A new approach to an old problem. *J Mol Biol* 1996;264:1164–1179. [PubMed: 9000638]
22. Simons KT, Bonneau R, Ruczinski I, Baker D. Ab initio protein structure prediction of CASP III targets using ROSETTA. *Proteins* 1999;(Suppl):171–176. [PubMed: 10526365]
23. Samudrala R, Levitt M. Decoys 'R' us: A database of incorrect conformations to improve protein structure prediction. *Protein Sci* 2000;9:1399–1401. [PubMed: 10933507]
24. Chiu TL, Goldstein RA. How to generate improved potentials for protein tertiary structure prediction: A lattice model study. *Proteins* 2000;41:157–163. [PubMed: 10966569]
25. Felts AK, Gallicchio E, Wallqvist A, Levy RM. Distinguishing native conformations of proteins from decoys with an effective free energy estimator based on the OPLS all-atom force field and the Surface Generalized Born solvent model. *Proteins* 2002;48:404–422. [PubMed: 12112706]
26. Seok C, Rosen JB, Chodera JD, Dill KA. MOPED: Method for optimizing physical energy parameters using decoys. *J Comput Chem* 2003;24:89–97. [PubMed: 12483678]

27. Tobi D, Elber R. Distance-dependent, pair potential for protein folding: results from linear optimization. *Proteins* 2000;41:40–46. [PubMed: 10944392]
28. Camacho CJ, Gatchell DW, Kimura SR, Vajda S. Scoring docked conformations generated by rigid-body protein–protein docking. *Proteins: Struct, Funct, Genet* 2000;40:525–537. [PubMed: 10861944]
29. Murphy J, Gatchell DW, Prasad JC, Vajda S. Combination of scoring functions improves discrimination in protein–protein docking. *Proteins: Struct, Funct, Genet* 2003;53:840–854. [PubMed: 14635126]
30. Sternberg MJ, Gabb HA, Jackson RM, Moont G. Protein–protein docking. Generation and filtering of complexes. *Methods Mol Biol* 2000;143:399–415. [PubMed: 11084916]
31. Gabb HA, Jackson RM, Sternberg MJ. Modelling protein docking using shape complementarity, electrostatics and biochemical information. *J Mol Biol* 1997;272:106–120. [PubMed: 9299341]
32. Holm L, Sander C. Evaluation of protein models by atomic solvation preference. *J Mol Biol* 1992;225:93–105. [PubMed: 1583696]
33. Mandell JG, Roberts VA, Pique ME, Kotlovyy V, Mitchell JC, Nelson E, Tsigelny I, Ten Eyck LF. Protein docking using continuum electrostatics and geometric fit. *Protein Eng* 2001;14:105–113. [PubMed: 11297668]
34. Eriksson AE, Baase WA, Wozniak JA, Matthews BW. A cavity-containing mutant of T4 lysozyme is stabilized by buried benzene. *Nature* 1992;355:371–373. [PubMed: 1731252]
35. Wei BQ, Baase WA, Weaver LH, Matthews BW, Shoichet BK. A model binding site for testing scoring functions in molecular docking. *J Mol Biol* 2002;322:339–355. [PubMed: 12217695]
36. Stahl M, Rarey M. Detailed analysis of scoring functions for virtual screening. *J Med Chem* 2001;44:1035–1042. [PubMed: 11297450]
37. Rarey M, Kramer B, Lengauer T, Klebe G. A fast flexible docking method using an incremental construction algorithm. *J Mol Biol* 1996;261:470–489. [PubMed: 8780787]
38. Verkhivker GM, Bouzida D, Gehlhaar DK, Rejto PA, Arthurs S, Colson AB, Freer ST, Larson V, Luty BA, Marrone T, Rose PW. Deciphering common failures in molecular docking of ligand-protein complexes. *J Comput-Aided Mol Des* 2000;14:731–751. [PubMed: 11131967]
39. Muegge I, Martin YC. A general and fast scoring function for protein–ligand interactions: A simplified potential approach. *J Med Chem* 1999;42:791–804. [PubMed: 10072678]
40. Ishchenko AV, Shakhnovich EI. Small Molecule Growth 2001 (SMoG2001): An improved knowledge-based scoring function for protein–ligand interactions. *J Med Chem* 2002;45:2770–2780. [PubMed: 12061879]
41. Gohlke H, Klebe G. Approaches to the description and prediction of the binding affinity of small-molecule ligands to macro-molecular receptors. *Angew Chem Int Ed* 2002;41:2644–2676.
42. Ferrara P, Gohlke H, Price DJ, Klebe G, Brooks CL 3rd. Assessing scoring functions for protein–ligand interactions. *J Med Chem* 2004;47:3032–3047. [PubMed: 15163185]
43. Morton A, Baase WA, Matthews BW. Energetic origins of specificity of ligand binding in an interior nonpolar cavity of T4 lysozyme. *Biochemistry* 1995;34:8564–8575. [PubMed: 7612598]
44. Su AI, Lorber DM, Weston GS, Baase WA, Matthews BW, Shoichet BK. Docking molecules by families to increase the diversity of hits in database screens: Computational strategy and experimental evaluation. *Proteins* 2001;42:279–293. [PubMed: 11119652]
45. Wei BQ, Weaver LH, Ferrari AM, Matthews BW, Shoichet BK. Testing a flexible-receptor docking algorithm in a model binding site. *J Mol Biol* 2004;337:1161–1182. [PubMed: 15046985]
46. Lorber DM, Shoichet BK. Flexible ligand docking using conformational ensembles. *Protein Sci* 1998;7:938–950. [PubMed: 9568900]
47. Meng EC, Shoichet BK, Kuntz ID. Automated docking with grid-based energy evaluation. *J Comput Chem* 1992;13:505–524.
48. McGovern SL, Shoichet BK. Information decay in molecular docking screens against holo, apo, and modeled conformations of enzymes. *J Med Chem* 2003;46:2895–2907. [PubMed: 12825931]
49. Kuntz ID, Blaney JM, Oatley SJ, Langridge R, Ferrin TE. A geometric approach to macromolecule–ligand interactions. *J Mol Biol* 1982;161:269–288. [PubMed: 7154081]

50. Shoichet BK, Kuntz ID. Matching chemistry and shape in molecular docking. *Protein Eng* 1993;6:723–732. [PubMed: 7504257]
51. Gschwend DA, Kuntz ID. Orientational sampling and rigid-body minimization in molecular docking revisited: on-the-fly optimization and degeneracy removal. *J Comput-Aided Mol Des* 1996;10:123–132. [PubMed: 8741016]
52. Li JB, Zhu TH, Cramer CJ, Truhlar DG. New class IV charge model for extracting accurate partial charges from wave functions. *J Phys Chem A* 1998;102:1820–1831.
53. Chambers CC, Hawkins GD, Cramer CJ, Truhlar DG. Model for aqueous solvation based on class IV atomic charges and first solvation shell effects. *J Phys Chem* 1996;100:16385–16398.
54. Pettersen EF, Goddard TD, Huang CC, Couch GS, Greenblatt DM, Meng EC, Ferrin TE. UCSF Chimera-A visualization system for exploratory research and analysis. *J Comput Chem* 2004;25:1605–1612. [PubMed: 15264254]
55. McGovern SL, Caselli E, Grigorieff N, Shoichet BK. A common mechanism underlying promiscuous inhibitors from virtual and high-throughput screening. *J Med Chem* 2002;45:1712–1722. [PubMed: 11931626]
56. McGovern SL, Helfand BT, Feng B, Shoichet BK. A specific mechanism of nonspecific inhibition. *J Med Chem* 2003;46:4265–4272. [PubMed: 13678405]
57. Lipscomb LA, Gassner NC, Snow SD, Eldridge AM, Baase WA, Drew DL, Matthews BW. Context-dependent protein stabilization by methionine-to-leucine substitution shown in T4 lysozyme. *Protein Sci* 1998;7:765–773. [PubMed: 9541409]
58. Otwinowski Z, Minor W. Processing of X-ray diffraction data collected in oscillation mode. *Macromol Crystallogr, A* 1997;276:307–326.
59. Brunger AT, Adams PD, Clore GM, DeLano WL, Gros P, Grosse-Kunstleve RW, Jiang JS, Kuszewski J, Nilges M, Pannu NS, Read RJ, Rice LM, Simonson T, Warren GL. Crystallography & NMR system: A new software suite for macromolecular structure determination. *Acta Crystallogr, Sect D: Biol Crystallogr* 1998;54:905–921. [PubMed: 9757107]
60. Su AI, Lorber DM, Weston GS, Baase WA, Matthews BW, Shoichet BK. Docking molecules by families to increase the diversity of hits in database screens: Computational strategy and experimental evaluation. *Proteins* 2001;42:279–293. [PubMed: 11119652]

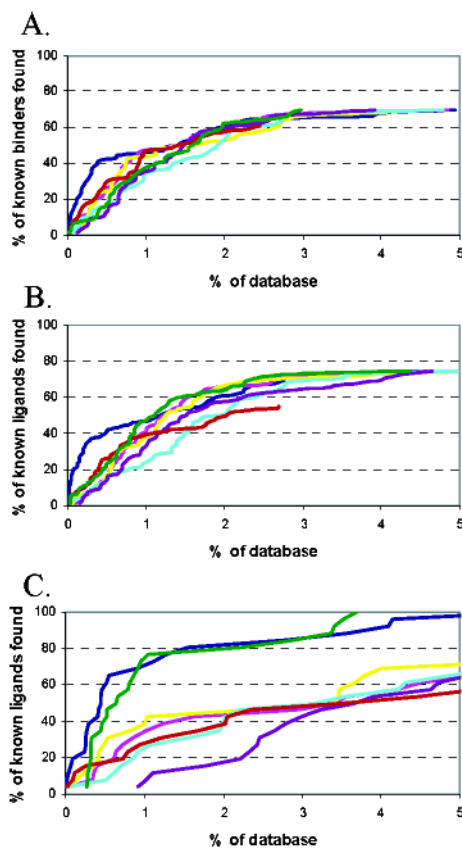


**Figure 1.** Protein targets used for “hit list” decoys. (A) Cavity binding site in L99A with benzene (carbons colored green) bound. (B) Cavity binding site in L99A/M102Q with phenol (carbons colored green) bound and forming a hydrogen bond (dashed line) with the O $\epsilon$ 2 oxygen of Gln102. In both A and B, the hydrophobic cavity is represented by a tan molecular surface. (C) Active site of AmpC with DOCK predicted pose of ligand 2 (Table 6). The ligand carbon atoms are colored green, three conserved water molecules are represented as red spheres, and hydrogen bonds are drawn with dashed lines. The figures were generated with PyMOL (DeLano Scientific LLC, San Carlos, CA).

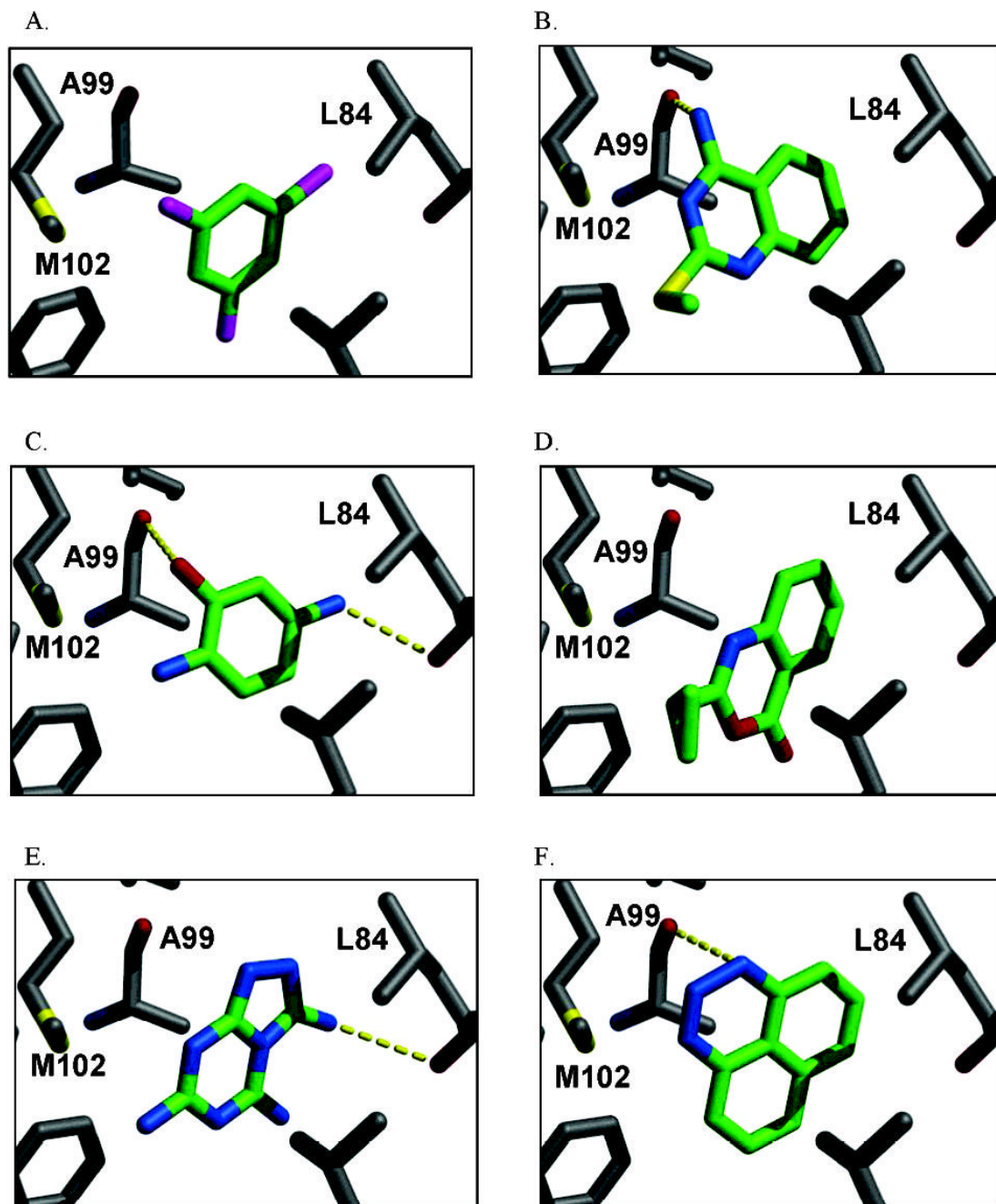


**Figure 2.** Catechol bound to L99A/M102Q at 1.55 Å resolution. The  $2F_o - F_c$  map is shown in blue wire frame at  $2\sigma$ , and the  $F_o - F_c$  electron density map (green) is contoured at  $3\sigma$ . The image was generated with PyMOL.



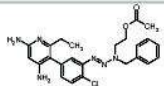
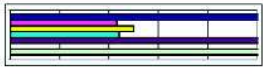
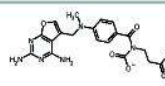
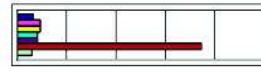
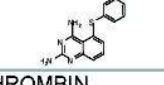
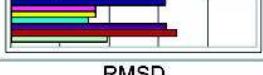
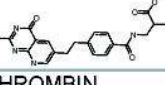

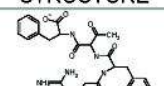

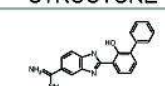

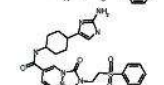
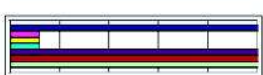
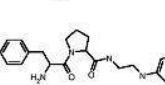
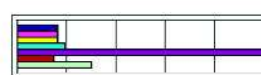
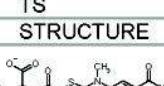
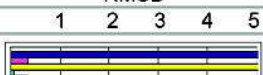
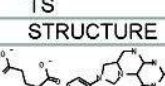
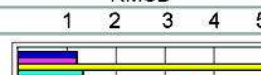
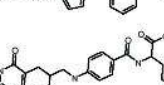

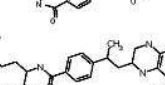
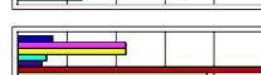
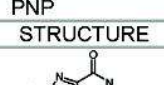
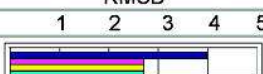
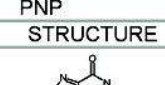
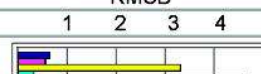
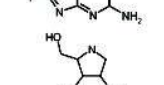

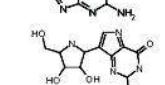

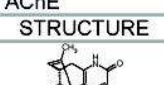
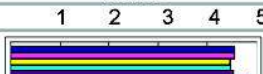
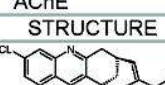

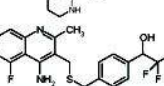

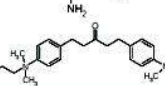



**Figure 3.** Enrichment of ligands for (A) L99A, (B) L99A/ M102Q, and (C) AmpC. The percentage of binders found (y-axis) at each percentage level of the ranked database using the entire ACD (x-axis). DOCK results are represented by the dark blue line, ScreenScore by magenta, FlexX by yellow, PLP by cyan, PMF by purple, SMOG by red, and the altered DOCK score with a softer 8–6 van der Waals potential and 4-fold increase in electrostatic score is plotted with the green line.



**Figure 4.** Characteristic high scoring docking hits to L99A by (A) DOCK (2nd ranking hit), (B) ScreenScore (1st ranking hit), (C) FlexX (1st ranking hit), (D) PLP (1st ranking hit), (E) PMF (1st ranking hit), and (F) SMOG (3rd ranking hit). The protein carbons are colored gray, and the carbons of the docked compounds are colored green. Hydrogen bonds are drawn with dashed lines. The images were generated with MidasPlus (UCSF, San Francisco, CA).

**Table 1**  
 Characteristic Geometric Decoys and Native-like Dockings Assessed by Different Scoring Functions

Geometric Decoys						Native-like Dockings							
DHFR		RMSD <sup>a</sup>				DHFR		RMSD					
LIGAND	STRUCTURE	1	2	3	4	5	LIGAND	STRUCTURE	1	2	3	4	5
TABA							MOT						
TQ3							DDF						
THROMBIN		RMSD				THROMBIN		RMSD					
LIGAND	STRUCTURE	1	2	3	4	5	LIGAND	STRUCTURE	1	2	3	4	5
ALG							130						
AIM							PPX						
TS		RMSD				TS		RMSD					
LIGAND	STRUCTURE	1	2	3	4	5	LIGAND	STRUCTURE	1	2	3	4	5
D16							TMF						
DHF							MTX						
PNP		RMSD				PNP		RMSD					
LIGAND	STRUCTURE	1	2	3	4	5	LIGAND	STRUCTURE	1	2	3	4	5
8IG							GUN						
IMR							IMG						
AChE		RMSD				AChE		RMSD					
LIGAND	STRUCTURE	1	2	3	4	5	LIGAND	STRUCTURE	1	2	3	4	5
HUB							HUX						
FBQ							EBW						

**Table 2**  
Characteristic L99A Experimentally Tested Ligands Scoring in the Top 10 000 Docking Hits and Their Ranks by Different Scoring Functions

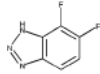
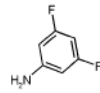
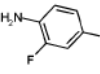
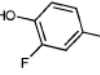
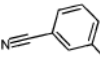
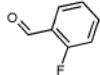
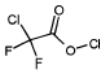
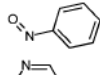
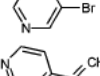
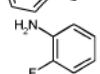
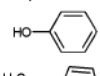
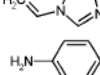
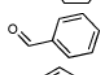
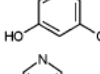
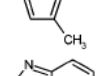
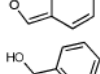
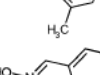
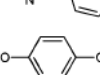



#	Ligands	Ranking by scoring function <sup>a</sup>						K <sub>d</sub> <sup>b</sup> ( $\mu$ M)
		D	S	F	PLP	PMF	S*	
1.		21	1156	1112	1961	7847	1826	NA
2.		25	949	1120	1273	1312	933	NA
3.		33	608	378	1417	2217	1725	102
4.		34	341	539	604	1046	793	470
5.		71	885	712	1580	3298	4586	NA
6.		83	323	585	177	344	274	193
7.		90	1368	616	3739	2682	NA	NA
8.		152	1625	765	4104	2861	3245	175
9.		182	676	1121	689	906	301	NA
10.		218	1304	709	3473	3887	NA	NA
11.		236	333	498	294	1292	2646	74
12.		302	1076	1346	1776	1345	662	68
13.		353	5310	4078	4475	6245	6338	NA
14.		363	339	473	310	515	1799	112
15.		365	360	509	325	264	842	290
16.		389	565	410	1019	1299	742	NA
17.		420	2464	2245	4099	2901	3563	NA
18.		518	1884	2238	2172	1842	942	422
19.		551	1381	1183	2670	5177	3203	NA
20.		616	535	743	146	2531	1943	NA
21.		627	5098	4139	4007	3073	3927	NA
22.		766	932	1494	1303	967	1559	364
23.		784	1770	3562	1311	1282	236	505
24.		1230	1475	1452	2882	2568	NA	NA
25.		1277	1261	1481	2568	3362	2813	NA
26.		2423	3104	4362	3135	2959	356	198

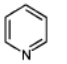
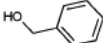

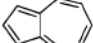
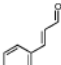
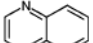
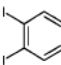
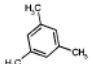

#	Ligands	Ranking by scoring function <sup>a</sup>						$K_d^b$ ( $\mu\text{M}$ )
		D	S	F	PLP	PMF	S*	
27.		2432	696	1212	614	3120	1866	NA
28.		2833	4261	5391	1934	1743	1755	NA
29.		2925	<b>139</b>	<b>193</b>	1153	539	<b>50</b>	NA
30.		3194	4928	5404	6544	1452	515	120
31.		3214	1593	1550	3816	2035	NA	NA
32.		3725	2899	3271	4193	1502	<b>156</b>	18
33.		3774	6394	7723	3897	2221	1065	NA
34.		4078	3246	2474	5358	1735	NA	NA
35.		4289	4055	5935	4892	4237	<b>395</b>	NA
36.		4704	3077	4838	3613	4939	1560	NA
37.		7787	9691	9424	9558	6699	4885	NA
38.		7923	4396	5597	5470	551	<b>75</b>	14
39.		9880	4098	5170	5474	1077	<b>92</b>	19

<sup>a</sup>D = DOCK, S = ScreenScore, F = FlexX, and S\* = SMOG (SMoG ranks are based on a ranking, which does not include halogenated compounds). Ranks in bold font indicate ligands, which rank in the top 500 for the respective scoring function.

<sup>b</sup>Experimentally determined  $K_d$  values ( $\Delta T_m$  values are known for ligands without a determined  $K_d$ ).<sup>43,60</sup> A full list of L99A ligands may be found in the Supporting Information and at <http://shoichetlab.combio.ucsf.edu/take-away.php>.

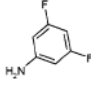
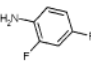
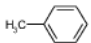

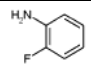
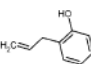
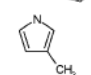

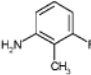
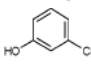
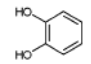
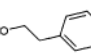
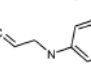
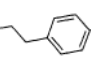
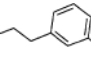
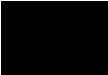
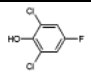


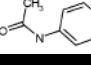

**Table 3**  
 Characteristic L99A Experimentally Tested Decoys Scoring in the Top 10 000 Docking Hits and Their Ranks by Different Scoring Functions

#	Decoys	Ranking by scoring function <sup>a</sup>					
		D	S	F	PLP	PME	S*
1.		46	748	685	658	999	NA
2.		88	998	441	2554	3374	NA
3.		91	869	400	2503	3976	NA
4.		112	1994	877	4854	4460	NA
5.		115	795	557	1393	1473	NA
6.		123	1046	889	1788	6035	NA
7.		125	8956	6911	9557	9756	NA
8.		126	1380	1136	2356	4221	3124
9.		164	1379	464	4655	1620	NA
10.		175	2610	2271	4031	813	2696
11.		222	737	283	1756	753	NA
12.		235	299	110	3127	3801	2641
13.		249	4761	4086	3214	4545	4403
14.		324	764	349	2387	1952	2559
15.		358	832	644	1543	3607	3072
16.		371	2235	1418	4613	4802	NA
17.		436	6769	5445	7392	8032	5044
18.		523	2217	3205	229	1883	2608
19.		607	1137	1872	1139	1950	1172
20.		611	1263	1324	1931	5213	1989
21.		642	1396	1012	2014	3814	1726



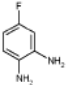
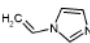
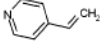
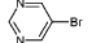
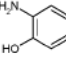
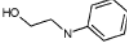
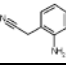
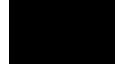
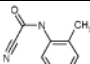
#	Decoys	Ranking by scoring function <sup>a</sup>					
		D	S	F	PLP	PME	S*
22.		671	1220	<b>493</b>	3593	1961	4847
23.		807	1635	1250	3594	4138	2077
24.		1379	4715	5126	2904	4493	3353
25.		2078	2001	4112	<b>40</b>	<b>107</b>	<b>130</b>
26.		2574	2755	3769	3476	580	1431
27.		2694	<b>50</b>	<b>119</b>	<b>264</b>	<b>27</b>	<b>402</b>
28.		5504	1804	1152	4670	4172	NA
29.		5936	2319	2774	4565	1388	<b>87</b>
30.		8243	6590	3362	9080	3544	NA

<sup>a</sup>D = DOCK, S = ScreenScore, F = FlexX, and S\* = SMOG (SMoG ranks are based on a ranking, which does not include halogenated compounds). Ranks in bold font indicate decoys, which rank in the top 500 for the respective scoring function. A full list of L99A decoys may be found in the Supporting Information and at <http://shoichetlab.compbio.ucsf.edu/take-away.php>.

**Table 4**  
 Characteristic L99A/M102Q Experimentally Tested Ligands and Decoys Scoring in the Top 10 000 Docking Hits and Their Ranks by Different Scoring Functions

#	Ligands	Ranking by scoring function <sup>a</sup>						K <sub>d</sub> <sup>b</sup> ( $\mu$ m)
		D	S	F	PLP	PME	S*	
1.		<b>8</b>	577	<b>332</b>	1200	1027	NA	NA
2.		<b>9</b>	<b>361</b>	<b>139</b>	939	5642	NA	NA
3.		<b>17</b>	1244	1082	2041	2257	2175	156
4.		<b>48</b>	1336	701	3191	8796	NA	NA
5.		<b>60</b>	<b>358</b>	<b>166</b>	780	848	NA	100
6.		<b>171</b>	3278	3708	2640	1430	511	NA
7.		<b>308</b>	4738	3169	7045	6720	5371	159
8.		<b>355</b>	1100	708	1857	3676	3857	90.9
9.		<b>417</b>	821	942	<b>421</b>	4318	NA	NA
10.		536	3026	2085	5969	5280	NA	56
11.		606	561	<b>419</b>	1573	4731	3594	NA <sup>c</sup>
12.		845	1185	1087	4285	4465	1214	NA
13.		979	1419	2765	1081	2017	751	NA
14.		1052	1067	1373	2956	7399	NA	NA
15.		1577	1495	1804	3132	2314	NA	NA
16.		2462	1503	1883	2197	1888	NA	NA
17.		2777	1380	734	5511	9286	NA	NA
18.		3557	2339	3144	2654	2550	1485	NA
19.		4277	1795	2541	4044	1403	<b>81</b>	NA
20.		4471	3808	3462	5322	4098	2649	NA
21.		4593	1150	1147	3436	<b>374</b>	<b>111</b>	NA



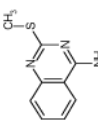
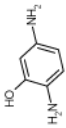
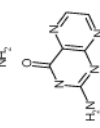
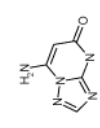
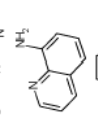
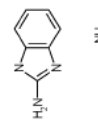
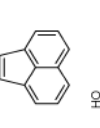
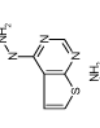
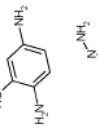
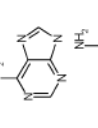
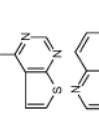
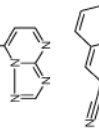
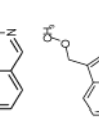
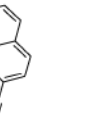
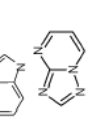
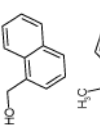
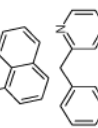


#	Ligands	Ranking by scoring function <sup>a</sup>					S*	K <sub>d</sub> <sup>b</sup> ( $\mu$ m)
		D	S	F	PLP	PME		
22.		5512	2034	1971	5544	2591	<b>323</b>	NA
1.		<b>28</b>	8531	6677	9212	9803	NA	
2.		<b>64</b>	<b>53</b>	<b>18</b>	<b>196</b>	3553	NA	
3.		<b>137</b>	4714	4188	2809	3791	5074	
4.		<b>152</b>	1740	1876	2304	1323	2970	
5.		<b>198</b>	1581	939	3271	1849	NA	
6.		<b>209</b>	<b>65</b>	<b>43</b>	503	1449	2216	
7.		1030	2248	3301	2456	4276	841	
8.		1451	1600	2167	1585	1394	744	
9.		3261	2908	3447	3057	2291	2446	
10.		7018	3641	3743	5584	3668	1091	

<sup>a</sup>D = DOCK, S = ScreenScore, F = FlexX, and S\* = SMOG (SMoG ranks are based on a ranking, which does not include halogenated compounds). Ranks in bold font indicate decoys, which rank in the top 500 for the respective scoring function.

<sup>b</sup>Experimentally determined K<sub>d</sub> values.<sup>35</sup>

<sup>c</sup> $\Delta T_m = 2.6$  °C. A full list of L99A/M102Q ligands and decoys may be found in the Supporting Information and at <http://shoichetlab.compbio.ucsf.edu/take-away.php>.

Decoys for L99A and L99A/M102Q Predicted by the ScreenScore, FlexX, PLP, PMF, and SMOG Scoring Functions; All Compounds Were Tested Experimentally

		L99A										L99A/M102Q									
#	Decoys	Ranking by scoring function <sup>d</sup>										Ranking by scoring function <sup>e</sup>									
		D	S	F	PLP	PMF	S*	#	Decoys	D	S	F	PLP	PMF	S*						
1.		9419	1	66	2	465	266	1.		571	5	2	288	621	1528						
2.		8241	4	12	35	40	2979	2.		987	3	10	112	28	1831						
3.		4568	40	150	137	3	435	3.		1941	7	12	41	64	827						
4.		7938	9	139	224	21	4	4.		2147	695	1926	1	5606	1718						
5.		699	6	1	799	734	1592	5.		2250	24	54	5	57	2169						
6.		1972	574	1756	5	6814	2552	6.		2275	1	6	33	10	1933						
7.		1424	11	19	56	209	1516	7.		9525	732	596	4709	232	2						
8.		7031	111	1349	4	1051	640														
9.		2513	10	7	134	199	2737														
10.		9520	423	694	1993	913	2														
11.		5537	76	280	391	550	3														
12.		9654	1162	3695	328	529	5														

<sup>d</sup>D = DOCK, S = ScreenScore, F = FlexX, and S\* = SMoG (SMoG ranks are based on a ranking, which does not include halogenated compounds). Ranks in bold font indicate decoys, which rank in the top 500 for the respective scoring function.

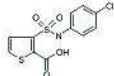

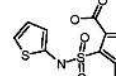
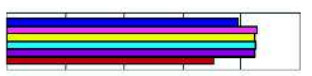
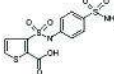
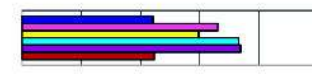
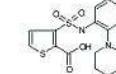
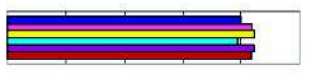
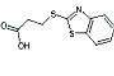

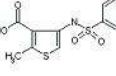
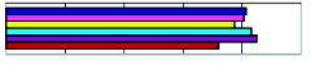


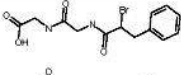

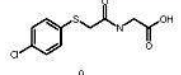

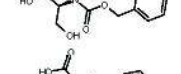

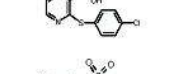

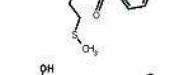

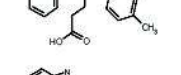

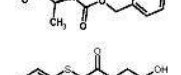



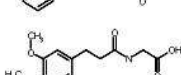



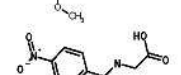

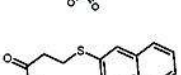

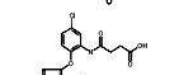
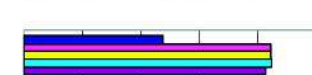
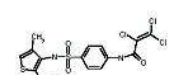

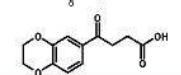
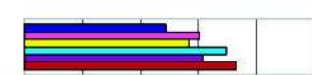




<sup>a</sup>Rank by scoring function. Blue = DOCK, magenta = ScreenScore, yellow = FlexX, cyan = PLP, purple = PMF, and red = SMoG (SMoG ranks are based on a ranking, which does not include halogenated compounds).

<sup>b</sup>The kinetic data for compounds **1** and **3-7** were reported previously.<sup>15</sup>

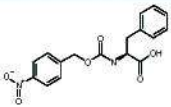

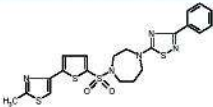
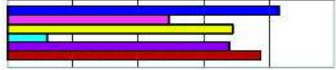
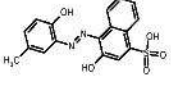
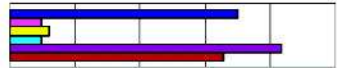
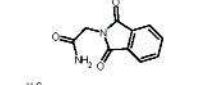
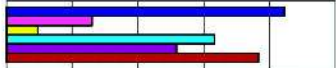
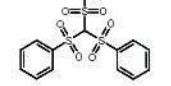

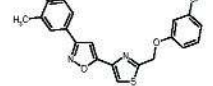
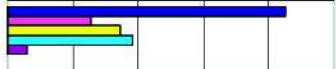
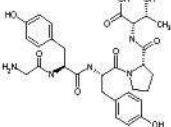

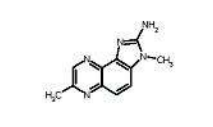
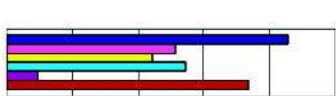
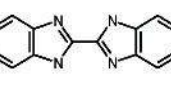
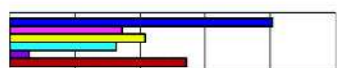
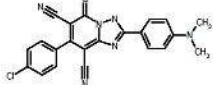
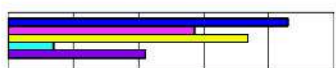
<sup>c</sup>An apparent  $K_i$  is reported for compound **2** assuming competitive inhibition and an IC<sub>50</sub> = 240  $\mu$ M. A full list of AmpC ligands and decoys may be found in the Supporting Information and at <http://shoichetlab.compbio.uesf.edu/take-away.php>.

<sup>a</sup>Rank by scoring function. Blue = DOCK, magenta = ScreenScore, yellow = FlexX, cyan = PLP, purple = PMF, and red = SMoG (SMoG ranks are based on a ranking, which does not include halogenated compounds).

**Table 6**  
 Charateristic AmpC Ligands and Decoys and Their Ranks by Different Scoring Functions

#	Ligands	RANKS <sup>a</sup>				K <sub>i</sub> <sup>b</sup> ( $\mu$ M)	#	Ligands	RANKS <sup>a</sup>				K <sub>i</sub> <sup>b</sup> ( $\mu$ M)
		10 <sup>1</sup>	10 <sup>2</sup>	10 <sup>3</sup>	10 <sup>4</sup>				10 <sup>1</sup>	10 <sup>2</sup>	10 <sup>3</sup>	10 <sup>4</sup>	
1.						26	5.						64
2.						93 <sup>c</sup>	6.						14
3.						646	7.						60
4.						318							
#	Decoys	RANKS <sup>a</sup>					#	Decoys	RANKS <sup>a</sup>				
		10 <sup>1</sup>	10 <sup>2</sup>	10 <sup>3</sup>	10 <sup>4</sup>			10 <sup>1</sup>	10 <sup>2</sup>	10 <sup>3</sup>	10 <sup>4</sup>		
1.							10.						
2.							11.						
3.							12.						
4.							13.						
5.							14.						
6.							15.						
7.							16.						
8.							17.						
9.													

**Table 7**  
Decoys for AmpC Predicted by the ScreenScore, FlexX, PLP, PMF, and SMOG Scoring Functions

#	Decoys	RANKS <sup>a</sup>				#	Decoys	RANKS <sup>a</sup>			
		10 <sup>1</sup>	10 <sup>2</sup>	10 <sup>3</sup>	10 <sup>4</sup>			10 <sup>1</sup>	10 <sup>2</sup>	10 <sup>3</sup>	10 <sup>4</sup>
1.						7.					
2.						8.					
3.						9.					
4.						10.					
5.						11.					
6.	